AN ACOUSTO-ULTRASONIC NDE TECHNIQUE FOR MONITORING MATERIAL ANISOTROPY

Hual-Te Chien, Shuh-Haw Sheen, and Apostolos C. Raptis
Materials and Components Technology Division
Argonne National Laboratory
Argonne, IL 60439

INTRODUCTION

Due to their higher strength-weight ratio, greater stiffness, stronger corrosion and wear resistance, longer fatigue life, and better thermal insulation, fiber-reinforced composite materials have been widely applied, for example, in the aerospace, automobile, marine, spacecraft, and construction industries. Evaluation of material properties, detection of defects, and prediction of life of these material is important but difficult. In the last decade, considerable attention has been focused on the use of acousto-ultrasonic (AU) and Leaky-Lamb wave techniques to evaluate material properties or changes in material properties due to fiber misorientation, flaws and defects, fiber/matrix debonding, or external loading [1-4]. A general summary of the AU approach, with bibliography, was presented by Vary [2]. A typical experimental setup with a personal computer (PC) used to analyze the AU waveforms was described by Kiernan and Duke [4]. Propagation of Leaky-Lamb waves in fiber-reinforced composites was investigated theoretically and experimentally by Chimenti and Nayfeh [10, 11]. A general discussion of elastic waves in solids can be found in Ref. 9.

To date, most studies have examined the available energy of the signal waveform (a combined waveform of bulk, extension, and Lamb waves) by measuring the stress wave factor (SWF), which requires sophisticated instrumentation and signal processing [1, 2, 4]. In this study, an alternative approach for AU nondestructive evaluation (NDE) that requires minimal instrumentation and analysis has been developed to monitor the material anisotropy of fiber-reinforced composites. Instead of measuring the SWF, the AU-wave time of flight (TOF) is measured and then related to material properties and fiber orientation. Two longitudinal transducers (0.5 MHz) are placed on the same surface of the composite to excite and catch Lamb waves. During excitation under the first critical frequency of the Lamb wave for the material, two fundamental modes are excited. The slower is the first antisymmetric mode and the faster is the first symmetric mode, which is nearly nondispersive and has a phase velocity very close to that of the bulk longitudinal wave. As the transducer separation increases, the measured time-domain AU signal of these two modes separates more distinctly.

The experiments were conducted with Kevlar 49, styles 120 and 181. The distance effect was also studied and shows that TOF dependence on transducer separation is linear. Thus, phase velocities, which depend strongly on fiber orientation with respect to wave propagation direction, in the media can be accurately determined from direct measurement of the TOF or from the slopes of the distance–effect curves. If the wave propagates away from the fiber direction, a slower but more attenuated wave is observed. Theoretical solutions of the bulk longitudinal wave are calculated by solving an eigenproblem with known material properties. Good agreement is obtained between experimental and theoretical results and shows that this technique is a better approach to determining material anisotropy than the SWF method. Because TOF is sensitive to the fiber orientation and fiber/matrix interface, this AU–NDE technique has great potential for detecting defects and debonding of fiber–reinforced composite materials.

THEORETICAL STUDY

Due to the anisotropic nature of composite materials, analysis of wave propagation in these materials is relatively complicated. The three–dimensional Hook's law must be considered in generating the three–dimensional wave equation. From the principle of conservation of energy for a homogeneous and anisotropic medium, acoustic fields in a solid are fully described by stress equations of motion, or so–called Christoffel equations, of a continuous medium with the absence of body forces [9],

$$\frac{\partial \sigma_{ij}}{\partial x_j} = \rho \frac{\partial^2 u_i}{\partial t^2}, \tag{1}$$

and the associated linear constitutive relations are

$$\begin{aligned} \sigma_{ij} &= C_{ijk\ell}\, \epsilon_{k\ell}, \\ \epsilon_{k\ell} &= \frac{1}{2}\left(\frac{\partial u_k}{\partial x_\ell} + \frac{\partial u_\ell}{\partial x_k}\right), \end{aligned} \tag{2}$$

where σ_{ij} represents the stress, $C_{ijk\ell}$ the elastic stiffness constant, ϵ_{ij} the strain, u_i the displacement, $i, j, k = 1, 2, 3$, ρ the material density, and $x_i = (x_1, x_2, x_3)$ the coordinate system.

If uniform plane waves are considered to propagate in a lossless unbounded (infinite) medium with the same wave numbers in all directions, the field is as follows:

$$u_j = U_j \exp^{i(\omega t - \xi I \cdot x_i)}, \tag{3}$$

where $I = (l_1 x_1, l_2 x_2, l_3 x_3)$ represents the unit vector of propagation direction, ξ the wave number, ω the circular frequency ($= 2\pi f$), and $i = \sqrt{-1}$. Substituting Eq. (3) into Eq. (1) yields three linear homogeneous coupled equations

$$(\Gamma_{ij} - \rho c^2 \delta_{ij}) u_j = 0, \tag{4}$$

where

$$\Gamma_{ij} = l_{ip} C_{pq} l_{qj}.$$

and $c = \omega/\xi$ is the phase velocity. l_{ip} is the gradient operator matrix and is given as

$$l_{pi} = \begin{bmatrix} l_1 & 0 & 0 & 0 & l_3 & l_2 \\ 0 & l_2 & 0 & l_1 & 0 & l_3 \\ 0 & 0 & l_3 & l_2 & l_1 & 0 \end{bmatrix}$$

with $l_{pi} = l_{ip}^{\mathrm{T}}$. The abbreviated subscript notations, or the so–called Vogit convention, are used to simplify the transformation of material constants and the matrix manipulations. These notations relate material constants C_{pq}, $p, q = 1, \ldots, 6$, to $C_{ijk\ell}$ with $1 \to 11$, $2 \to 22$, $3 \to 33$, $4 \to 23$, $5 \to 13$, and $6 \to 12$, respectively.

By solving the eigenproblem in Eq. (4), the bulk–wave velocities associated with a longitudinal wave (P–wave) and two shear waves (SH and SV–waves) can be obtained. If the medium has a finite thickness d, and the plane waves propagating

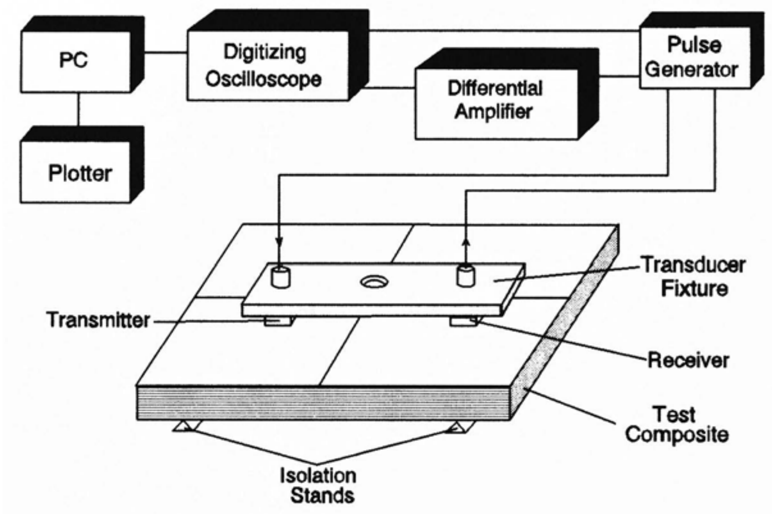

Fig. 1 Experimental configuration of acousto–ultrasonic system.

along the x_1-direction are independent of x_2, the phase velocities of the Lamb waves can be obtained by solving Eq. (4) and simultaneously satisfying the associated boundary conditions, i.e., free surface traction on both surfaces of the media [10, 11]. The phase velocities of the Lamb waves are dispersive to the frequency and also the azimuthal angle. However, by holding the frequency below that of the first critical frequency, only two fundamental Lamb modes can be detected: one is the first antisymmetric mode with lower phase velocity, which is dispersive but not sensitive to the changing of azimuthal angle; the another is the first symmetric mode with higher velocity, which is nearly nondispersive and very close to that of the associated bulk longitudinal wave, and is also sensitive to the changing of azimuthal angle. Therefore, in this study we compare the experimental measurements only with the theoretical results for the bulk longitudinal wave.

EXPERIMENTAL PROCEDURE

Because only TOF is measured in this experiment, the experimental setup and signal processing are much simpler than those needed for the SWF method. In this experiment, a Wavetek pulse generator is used to excite a longitudinal–wave, or P–wave, transducer with a pulse width of 1.2 μsec. Two transducers, one acting as a transmitter and the another as a receiver, are attached normal to the surface on the same side of the composite, with a well–defined separation distance between the transmitter and receiver (DTR). Both transducers have a center frequency of 0.5 MHz and are with 0.5 in. in length and 1.0 in. in width. To obtain a good signal within a reasonably accessible space, the separation distance is chosen as 3 in. The received signal is magnified by a differential AC amplifier before being sampled and displaced on a LeCroy 9400 digital oscilloscope. The complete experimental setup is illustrated in Fig. 1.

Due to the highly attenuated nature and material anisotropy of composites, the surface smoothness, couplant condition, and pressure of the transducer attachment must be examined and established before the experiment. In most cases, surface finishing was not necessary because the composite surface was adequately smooth due to its surface coating. Ultragel couplant was used to attach the transducers. To maintain consistency in the TOF readings, a constant pressure was loaded on both

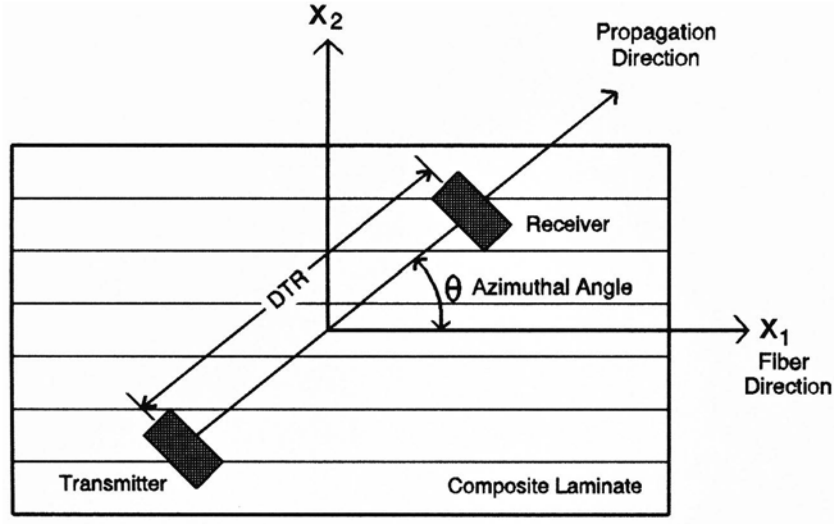

Fig. 2 Fiber orientation and setup.

transducers. A distance–measurement fixture was used to house the transducers at selected separations.

The line joining the transmitter and the receiver is defined as the wave propagation direction. In Fig. 2, the x_1-axis defines the direction that is parallel to the 0° fiber orientation of the specimen, and the angle between the propagation direction and the x_1-axis is called the azimuthal angle, Θ. Figure 2 also shows the fiber orientation and setup of the composite. A 360° protractor is placed on the transducer fixture to establish the azimuthal angle. The linear readings of the TOF were taken from the average of 500 samplings. Phase velocities were then obtained by collecting TOF at different azimuthal angles to show material anisotropy. Scans on both sides of the composite were made to verify experimental consistency, and we found that the data obtained from one side of the composite were accurate enough to identify the material anisotropy. The distance effect was also studied by measuring the TOF with variations of DTR for a fixed azimuthal angle. The slopes of the TOF curve were then related to the phase velocities of the longitudinal bulk wave.

RESULTS AND DISCUSSION

Experiments were conducted for Kevlar 49 (styles 120 and 181) composites to demonstrate this AU technique. Style 120, is a composite having 28 plies in the warp direction with plain weave in Fiberite MXM7714 resin, while style 181 has 11 plies in the warp direction with 8–harness satin weave in Cucom 919 resin. Both styles are bidirectional composites and their material properties are

$$C_{11} = C_{22} = 40.09 \text{ GPa}, \quad C_{33} = 5.54 \text{ GPa},$$
$$C_{12} = 1.88 \text{ GPa}, \quad C_{13} = C_{23} = 1.68 \text{ GPa},$$
$$C_{44} = C_{55} = 2.1 \text{ GPa}, \quad C_{66} = 2.3 \text{ GPa}, \quad \rho = 1.6 \text{ g/cm}^3.$$

Figure 3 shows the AU waveforms for style 120 measured with DTRs of 3 and 8 in. A clear separation of these two groups is observed when DTR is 8 in. The distance–dependent TOFs for both Kevlar styles are given in Fig. 4, and the results show that the dependence of TOF on transducer separation is linear. Therefore, from the inverse of the slope of the linear dependences, the phase velocities of the longitudinal bulk wave for various azimuthal angles are determined. However, because the transducers are 0.5 in. in length, the TOF for DTR $\leq$ 1.5 in. is difficult to resolve. Furthermore, the linear line does not cross the origin, chiefly because the process is no longer of the AU mode but is under a pulse–echo mode. The slope for

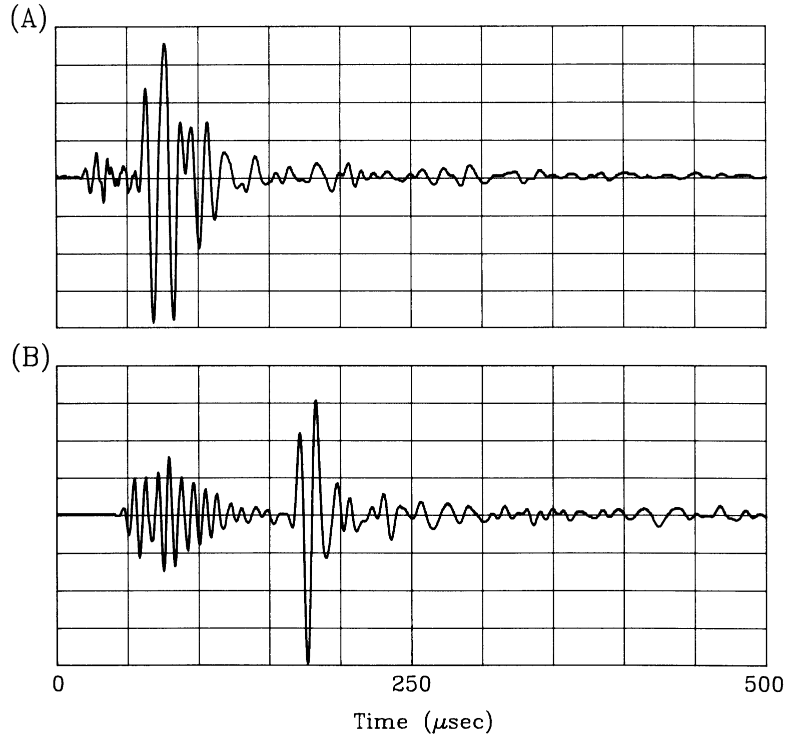

Fig. 3 AU waveforms for Kevlar 49, style 120, composite panel at (A) DTR = 3 and (B) DTR = 8 inches.

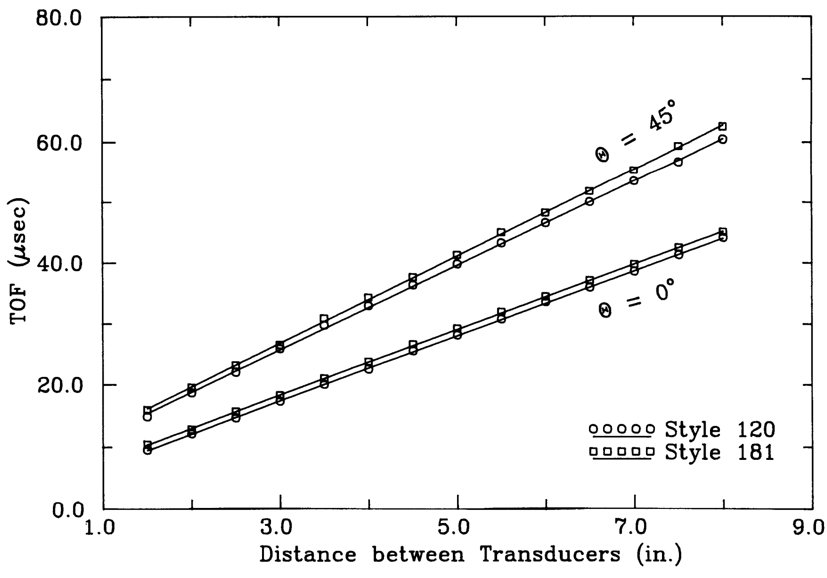

Fig. 4 Distance effect for Kevlar 49, styles 120 and 181, composite panels at $\Theta = 0°$ and 45°.

Table 1 Phase velocities of Kevlar 49, styles 120 and 181, composites from TOF and slope measurements, and theoretical approaches, respectively (Unit: km/sec).

Approach Method	*Kevlar 49 120*		*Kevlar 49 181*	
	0°	45°	0°	45°
TOF	4.882	3.892	4.806	3.762
Slope	4.908	3.666	4.798	3.579
Theory	5.006	3.815	5.006	3.815

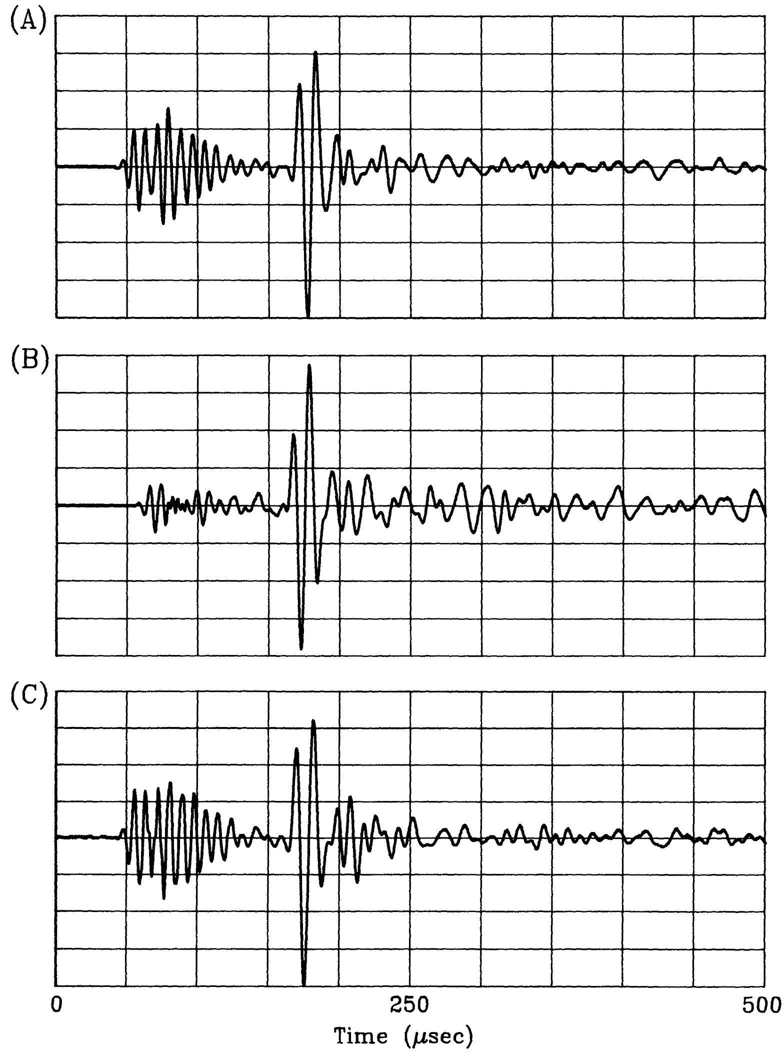

Fig. 5 AU waveforms for Kevlar 49, style 120, composite panel at (A) $\Theta = 0°$, (B) $\Theta = 45°$, and (C) $\Theta = 90°$, respectively.

wave propagation along $\Theta = 0°$ is smaller than that along 45°; thus, the phase velocity in 0° is greater than that in 45°. This can also be verified by examining the AU waveform TOF.

Under the first critical frequency, two Lamb modes were generated: one is the first antisymmetric mode with a lower velocity; the another is the first symmetric

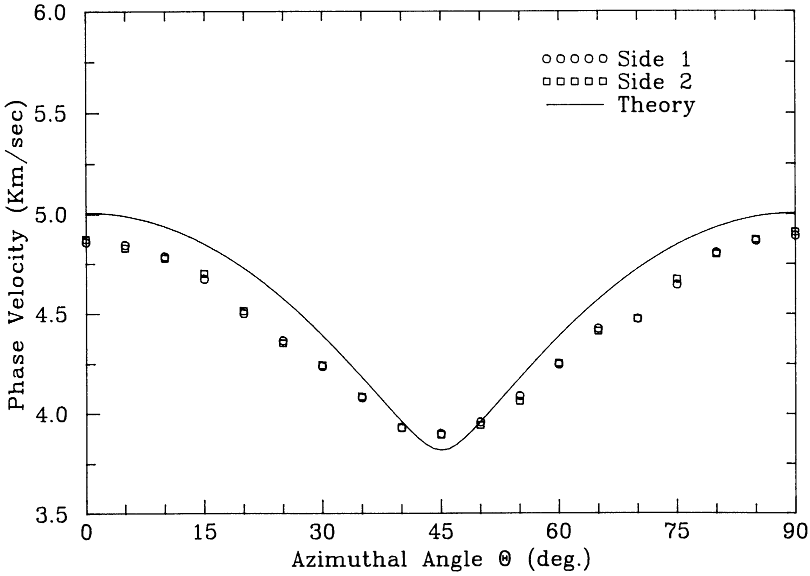

Fig. 6 Effect of fiber orientation for Kevlar 49, style 120, composite panel.

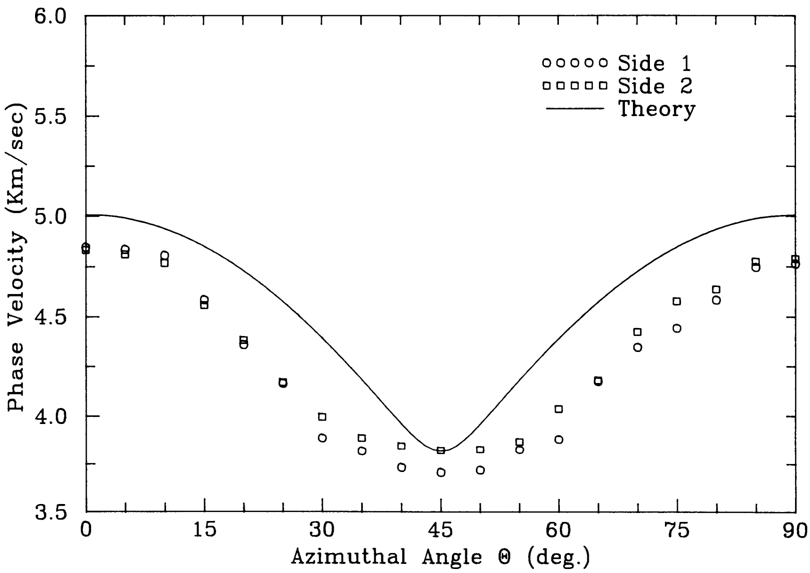

Fig. 7 Effect of fiber orientation for Kevlar 49, style 181, composite panel.

mode with a higher velocity. If the ultrasonic waves propagate away from the fiber direction, these two modes still can be observed but they travel at a lower velocity and display a higher attenuation. Figure 5 shows the waveforms for $\Theta = 0°$, 45°, and 90° for a style 120, composite with a DTR of 3 in. Because the composite has bidirectional symmetry, the waveforms for $\Theta = 0°$ and 90° are similar and have TOFs of 14.92 and 14.83 μsec, respectively. If $\Theta = 45°$, the signal suffers higher attenuation and also shows a slower TOF of 18.14 μsec. Therefore, the TOF of an AU waveform is dispersive with respect to the azimuthal angle. Because TOF and attenuation of AU signals may be related to fiber direction and bonding condition, it is possible to use this AU–NDE technique to study the fiber/matrix interface, debonding and defects, and effects of external loading.

Such phase–velocity versus azimuthal–angle curves for both sides of the style 120 composite panel are given in Fig. 6, along with the theoretical results obtained by solving the eigenfunction in Eq. (4) if the material properties are defined. Figure 7 gives the phase–velocity curves and theoretical results for the style 181 composite panel. Good agreement between theoretical results and experimental data is obtained, and the phase–velocity measurements based on the phase–velocity curves from both sides of a composite and on the slope of linear curves from the distance effect show high accuracy and consistency. Table 1 shows a summary of the phase velocities obtained from these three approaches for the Kevlar 49 composite materials measured at $\Theta = 0°$ and 45°. The TOF approach is easier to use in obtaining phase velocity and the dispersion curve, while the slope approach requires measurements at different locations but gives better results. Differences between the experimental and theoretical results may be due to slight variations in the material constants and the TOF measurements. A more sophisticated method for measuring TOF should be used, but agreement is nevertheless still good.

CONCLUSIONS

A simpler and better way of monitoring the anisotropy of fiber–reinforced composite materials, based on the acousto–ultrasonic approach, is presented. In this approach, time of flight of the acousto-ultrasonic waves, rather than the stress wave factor, is measured. Two fundamental Lamb modes are generated under the first critical frequency: one is the first antisymmetric mode traveling with a lower velocity, while the other is the first symmetric mode traveling at a higher velocity. The latter is sensitive to azimuthal angle and is nearly nondispersive, and has a phase velocity very close to that of the bulk longitudinal wave of the material. Experimental data measured by two approaches, TOF measurement and slope method, are compared with the theoretical results; good agreement is obtained for the material anisotropy. There is a great potential for this AU approach in material–property evaluation and in quantitative measurement of defects and debonding of fiber–reinforced composites. However, more studies are needed to better understand the effect of the fiber/matrix bonding on the measurements and to extract more information from the AU signals.

ACKNOWLEDGMENT

Work sponsored by U.S. Department of Energy/Fossil Energy/Advanced Research Technology Development/Materials Program, under Contract W-31-109-Eng-38.

REFERENCES

1. J. C. Duke, Jr., editor, *Acousto–Ultrasonics – Theory and Application* (Plenum Press, New York, 1988).
2. A. Vary, Matl. Eval. 49, 581 (1991).
3. V. K. Choo, S.–H. Sheen, W. P. Lawrence, and H.–T. Chien, in *Proceedings of the First Canadian International Composites Conference and Exhibition* (Montreal 1991).
4. V. K. Choo, S.–H. Sheen, W. P. Lawrence, and H.–T. Chien, in *SAMPE Technical Seminar* (Fort Worth/Dallas, USA, 1991).
5. A. Vary, in *Non–destructive Testing of Fiber–Reinforced Plastics Composites*, edited by John Summerscales (Elsevier Applied Science, UK), p. 1 (1991).
6. M. T. Kiernan and J. C. Duke, Jr., Matl. Eval. 46, 1344 (1988).
7. D. E. Chimenti and A. H. Nayfeh, J. Appl. Mech., Trans. ASME 33, 4531 (1985).
8. A. H. Nayfeh and D. E. Chimenti, J. Acoust. Soc. Am. 83, 1736 (1988).
9. B. A. Auld, *Acoustic Fields and Waves in Solids*, Vols. I & II (John Wiley, New York, 1973).